厚生労働科学研究費補助金（第３次対がん総合戦略研究事業）

厚生労働省科学研究費補助金（第3次対がん総合戦略研究事業）
遺伝子不安定性の機能解析及び遺伝子変異推測モデルの構築による
乳癌卵巣癌ハイリスクキャリアーの同定と発症予防法の確立

卵巣癌特異的染色体異常やヘテロ接合性消失のゲノム網羅的同定に関する研究

分担研究者　井ノ上 逸朗　東海大学医学部 基礎医学系　教授

研究要旨

卵巣癌や乳癌は、他の癌種と同様、細胞遺伝学的異常を伴うことが知られているものの、染色体不安定性に関わる遺伝要因が十分明らかになっているとはいえない。昨年度までは、卵巣癌および乳癌ゲノムにつき、それぞれに特異的な染色体構造異常領域の体系的同定に取り組んだ。本年度は、これまでに得た知見の一般性評価を主たる目的として、卵巣癌、乳癌の検体追加およびゲノム網羅的検索を実施した。本研究課題において取得した網羅的染色体構造異常データは、染色体不安定性という観点から各癌種を特徴付けるための重要な基盤となることが期待される。

A. 研究目的

卵巣癌や乳癌は、通常、染色体の異数化などの細胞遺伝学的異常を伴うことが知られている。本年度も、昨年度からの継続として、卵巣癌、乳癌特異的ゲノム構造変化領域を体系的に同定することを目的とする。より一般性の高い知見を得るために、それぞれの癌種において、孤発性症例からのサンプルを追加し、SNP アレイとよばれるゲノム網羅性の高いマイクロアレイを用いて、癌ゲノム特異的染色体構造異常領域をゲノム全域から体系的に検索した。

B. 研究方法

昨年度までと同様、ゲノム網羅的検索のために、Genome-Wide Human SNP Array 5.0 (Affymetrix 社)および Partek Genomics Suite 6.4 ソフトウェア (Partek 社)を使用した。卵巣癌および正常組織（16 対応対サンプル）、乳癌および正常組織（*BRCA1* 変異陽性；1 対応対

サンプル）から抽出したゲノム DNA を用いて、ゲノム構造変化を高密度に分析した。

（倫理面への配慮）

新潟大学、東海大学ほか、本研究への協力研究機関それぞれの機関内倫理審査委員会にて患者組織の採取、癌細胞および正常細胞由来 DNA を用いた研究について承認を得ている。個人情報管理者による適切な情報管理のもと研究を遂行しており、研究実施施設（東海大学医学部）には個人情報は一切存在しない。

C. 研究結果および考察

正常ゲノムにおける平均 SNP 遺伝子型コール率は 99%超であり、信頼性の高いデータが取得されたと考えた。

次に、癌–正常対サンプルにおける比較解析から、追加サンプルにおいても、多数の癌ゲノム特異的構造変化を見いだした（図1および2）。卵巣癌、乳癌特異的変化はいずれも、1コピー重複や欠失といったアレル特異的コピー数変化がその多数を占めるという共通性を有することが明らかになった。他方、乳癌ゲノムは、卵巣癌のそれと比し、癌ゲノム特異的構造変化領域の頻度（度数）が低い傾向を示し、同じ固形癌であっても、癌種によって、染色体構造変化の度合いが異なる可能性を認めた。

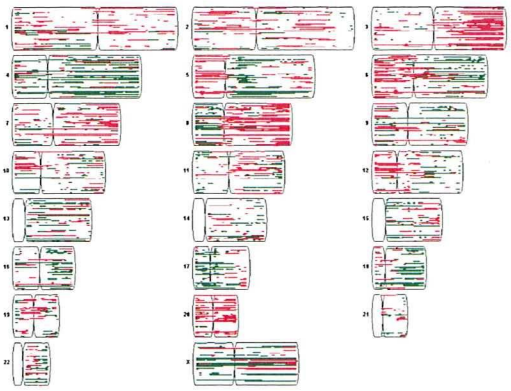

図1 卵巣癌–正常ゲノム対比較からの染色体構造異常領域マップ（重複：赤色、欠失：緑色）

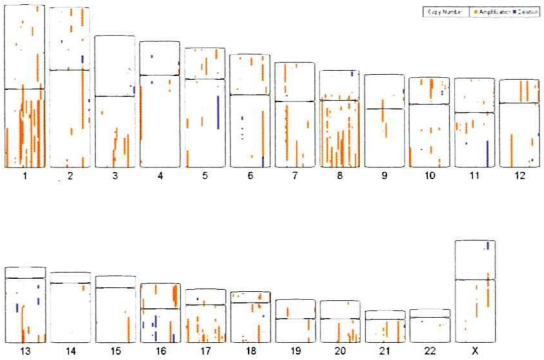

図2 乳癌–正常ゲノム対比較からの染色体構造異常領域マップ（重複：赤色、欠失：青色）

E. 結論

本研究課題では、卵巣癌 59 サンプル、乳癌 38 サンプルにつき、各癌ゲノム特異的な構造異常領域を明らかにし、カタログ化することができた。染色体不安定性という観点から、それぞれの癌を特徴付けるための重要な基盤となることが期待される。

F. 健康危険情報

特記事項なし。

G. 研究発表

1)論文発表

1. Sekigawa T, Tajima A, Hasegawa T, Hasegawa Y, Inoue H, Sano Y, Matsune S, Kurono Y, Inoue I. Gene-expression profiles in human nasal polyp tissues and identification of genetic susceptibility in aspirin intolerant asthma. *Clin Exp Allergy* 39, 972-981, 2009.
2. Kang E-H, Yamaguchi T, Tajima A, Nakajima T, Tomoyasu Y, Watanabe M, Yamaguchi M, Park S-B, Maki K, Inoue I. Association of the growth hormone receptor gene polymorphisms with mandibular height in a Korean population. *Arch Oral Biol* 54, 556-562, 2009.
3. Tomoyasu Y, Yamaguchi T, Tajima A, Nakajima T, Inoue I, Maki K. Further evidence for an association between mandibular height and the growth hoemone receptor genes in a Japanese population. *Am J Orthod Dentofacial Orthop* 136, 536-541, 2009.
4. Koike A, Nishida N, Inoue I, Tsuji S, Tokunaga K. Genome-wide association database developed in the Japanese Integrated Database Project. *J Hum Genet* 54, 543-546, 2009.
5. Ruigrok YM, Rinkel GJ, Wijmenga C, Kasuya H, Tajima A, Takahashi T, Hata A, Inoue I, Krischek B. Association analysis of genes involved in the maintenance of the integrity of the extracellular matrix with intracranial aneurysms in a Japanese cohort. *Cerebrovasc Dis* 28, 131-134, 2009.
6. Brookes AJ, Lehvaslaiho H, Muilu J, Shigemoto Y, Oroguchi T, Tomiki T, Mukaiyama A, Konagaya A, Kojima T, Inoue I, Kuroda M, Mizushima H, Thorisson GA, Dash D, Rajeevan H, Darlison MW, Woon M, Fredman D, Smith AV, Senger M, Naito K, Sugawara H. The phenotype and genotype experiment object model (PaGE-OM): a robust data structure for information related to DNA variation. *Hum Mutat* 30, 968-977, 2009.
7. Nakaoka H, Inoue I. Meta-analysis of genetic association studies: methodologies, between-study heterogeneity and winner's curse. *J Hum Genet* 54, 615-623, 2009.
8. Yoshihara K, Tajima A, Komata D, Yamamoto T, Kodama S, Fujiwara H, Suzuki M, Onishi Y, Hatae M, Sueyoshi K, Fujiwara H, Kudo Y, Inoue I, Tanaka K. Gene expression profiling of advanced-stage serous ovarian cancers distinguishes novel subclasses and implicates *ZEB2* in tumor progression and prognosis. *Cancer Sci* 100, 1421-1428, 2009.
9. Yoshihara K, Tajima A, Yahata T, Kodama S, Fujiwara H, Suzuki M, Onishi Y, Hatae M. Sueyoshi K, Fujiwara H, Kudo Y, Kotera K, Masuzaki H, Tashiro H, Katabuchi H, Inoue I, Tanaka K. Gene expression profile for predicting survival in advanced-stage serous ovarian cancer

across two independent databases. *PLoS ONE* 5, e9615, 2010.

2) 学会発表

1. Yoshihara K, Tajima A, Adachi S, Komata D, Yamamoto T, Kodama S, Fujiwara H, Suzuki M, Onishi Y, Hatae M, Sueyoshi K, Fujiwara H, Kudo Y, Inoue I, Tanaka K: Gene expression profile identified novel subclasses in advanced-stage serous ovarian cancers and revealed *ZEB2* expression as the prognostic marker. AACR 100th Annual Meeting 2009, Denver, USA. April 18-22, 2009.
2. 田嶋敦、吉原弘祐、井ノ上逸朗、田中憲一：漿液性卵巣癌における DNA コピー数および遺伝子発現量変化に関する統合ゲノミクス解析. 日本人類遺伝学会第 54 回大会. 東京. 2009.9.23-26.

H. 知的財産権の出願、登録状況

1.特許取得

なし。

2.実用新案登録

なし。

3.その他

なし。

厚生労働科学研究費補助金（第３次対がん総合戦略研究事業）
分担研究報告書

遺伝子不安定性の機能解析及び遺伝子変異推測モデルの構築による乳癌卵巣癌ハイリスクキャリアーの同定と発症予防法の確立

研究分担者　佐伯　俊昭　埼玉医科大学　教授

研究要旨
目的：日本人乳がんにおける BRCA1 の意義と、NSABP/GAIL model による発症相対危険度を対比するために、日本人乳癌の生物学的特性をサブクラスと BRCA1､2 の発現との関連性について検討した。対象と方法：乳がん 25 症例の遺伝子検索を行った。方法は、DNA micro array により解析した。解析が可能であった 22 例中、luminal A;5 例, B;8 例, HER２ enrich;4 例, Basal like;5 例であった。各 subtype の BRCA1,2 の発現率の中央値は、それぞれ A;85.3, 76.4, B;59.3, 51.3, HER２;82.6, 83.8, Basal like;78.2, 79.0 であった。Basal like 全例が再発 high risk であり、また変異は２例に認められたが、症例が少なく intrinsic subtype との関連は不明であった。NSABP/GAIL model の評価が可能であった 2 例ではいずれも BRCA1 の遺伝子発現を有しない症例に比較し、相対危険率が高い傾向にあった。日本人乳がんの特徴は、intrinsic subtype と対比した BRCA1,2 の発現から、ほぼ白人と同様の可能性が推測された。

A. 研究目的

日本人乳がんの Intrinsic subtype の luminal A と Luminal B の割合は白人と異なり、また Basal like に多く発現する BRCA1 を含む遺伝子的な特徴が異なることが示唆されている。日本人乳がんの家族集積性における BRCA1 の意義と、白人乳がんリスクモデルで

あるNSABP/GAILmodelによる発症相対危険度について関連を検討する。

B. 研究方法

2009年当院の手術症例25例を対象に、乳がん組織での DNA-microarrayによるBRCA1,2の発現を検討した。また同時に、subtypeに分類するためにEstrogen receptor(ER), PgR(progesterone receptor), HER 2についても同時に測定した。Lunimal Aは、ERor PgR 陽性、HER2 陰性、低増殖能、B は ERor PgR 陽性、HER2 陰性、高増殖能、Basal likeは ER and PgR 陰性、HER2 陰性とした。解析方法は、373 例の乳がん組織における各遺伝子の発現を log scale で求め、対象症例の発現が、373症例のどの分布に位置するかを relative expression percentile (相対発現率) として求めた。

(倫理面への配慮)

説明同意文書にて組織採取の承諾を得た。また、研究対象者の識別は匿名化し、解析に用いた。乳がん患者の問診票から得られた情報を使用した。以上の資料は鍵がかかる保管庫で責任者を決め保管した。

C. 研究結果

25例中22例にmicro arrayによる解析が可能であった。25例中3例は解析に必要なRNAが不足、あるいは変性していた。22例中、luminal A;5, B;8, HER2 enrich;4, Basal like;5であった。各subtypeのBRCA1,2の発現率の中央値は、それぞれ A;85.3,76.4, B;59.3,51.3, HER 2 ;82.6,83.8, Basal like;78.2,79.0 であった。Basal like全例が再発high riskであった。また変異は2例に認められたが、症例が少なくintrinsic subtypeとの関連は不明であった。NSABP/GAIL modelの評価が可能であった2例ではいずれもBRCA1の遺伝子発現を有しない症例に比較し、相対危険率が高い傾向にあった。

D. 考察

乳がん発症の初期にBRCA1の変異が大きく関与していると報告されるが、乳腺組織におけるDNA repair gene発現が高いと、その発がんプロセスにおける変異の相対的な意義については不明である。あくまでも乳がん組織を用いた研究であるが、日本人乳がんにおけるBRCA1発現率はluminal BおよびBasal likeに高い傾向にあり、白人と同様のintrinsic subtypeである可能性が支持された。

E. 結論

日本人乳がんの特徴は、intrinsic subtypeと対比したBRCA1,2の発現から、ほぼ白人と同様の可能性が推測されたが、Luminal Bはがん幹細胞の分化の完成された時期、またBasal likeは分化の初期に相当すると考えられているサブタイプであり、BRCA1,2の発現が乳がんの発症と分化度に関連していると推測された。発症リスクのデータが不足しており、遺伝子発現と

の関連は現在解析中である。

F. 健康危険情報

特になし

G. 研究発表

1. 論文発表

①Saeki T., et al., Pharmacokinetic analysis of a combined chemoendocrine treatment with paclitaxel and toremifene for metastatic breast cancer. Breast Cancer 16:113-120 2009

②Saeki T., et al., Evaluation of the safety and tolerability of oral TAS-108 in postmenopausal patients with metastatic breast cancer. Annals of Oncology 20(5):868-873 2009

③Saeki T., et al., Physiological and oncogenic aurora-pathway. International Journal of Biological Sciences 5(7):722-726 2009

④ Okita A., Saeki T., et al., Efficacy and tolerability of weekly paclitaxel combination with high-dose toremifene citrate in patients with metastatic breast cancer. Acta Medica Okayama 63(4):187-194 2009

⑤Omokawa Y., Saeki T., et al., In vitro and in vivo anti-tumor effects of novel Span 80 vesicles containing immobilized Eucheuma serra aggulutinin. International Journal of Pharmaceutics, in press, 2010

2. 学会発表

H. 知的財産権の出願・登録状況

1. 特許取得　該当なし
2. 実用新案登録　該当なし
3. その他　該当なし

別紙４

研究成果の刊行に関する一覧表

雑誌

発表者氏名	論文タイトル名	発表誌名	巻名	ページ	出版年
Masayuki Yamaguchi, Tetsuro Yahata, Kazuyuki Fujita, Junko Sakurada, Hajime Umezu Kenichi Tanaka	Extranodal Rosai-Dorfman Disease Involving Bilateral Ovaries in a Patient with a Venticuloperitoneal Shunt	J Obstet Gynaecol Res	35(5)	1000-1003	2009
Yoshihara K, TajimaA, Komata D, YamamotoT, Kodama S, Fujiwara H, Suzuki M, Onishi Y. Hatae M, Sueyoshi K, Fujiwara H, Kudo Y, Inoue I. Tanaka K	Gene expression profiling of advanced-stage serous ovarian cancers distinguishes novel subclasses and implicates ZEB2 in tumor progression and prognosis.	Cancer Sci	100(8)	1421-8	2009
Quan J, Yahata T, Tamura N, Nagata H Tanaka K .	Relationship between single nucleotide polymorphisms in CYP1A1 and CYP1B1 genes and the bone mineral density and serum lipid profiles in postmenopausal J apanese women taking hormone therapy.	Menopause.	16(1)	171-6	2009
Kyoko Yamada, Kazuyuki Fujita. Jinhua Quan, Masayuki Sekine Katsunori Kashima, Tetsuro Yahata, Kenichi Tanaka	Increased apoptosis of germ Cells in patients with AZFc deletions	J Assist Reprod Genet		In press	2010
C. Banzai, T. Yahata, K. Fujita, Y. Ajioka, M. Kawahara, H. Okamura K. Tanaka	Recurrent borderline ovarian tumor presenting as a pedunculated polyp at colonoscopy	Endoscopy	42	69-70	2010

Dai komata, Tetsuro Yahata,Shoji Kodama, Yu koyama, Nobuo Takeda, Kenzo Tajima Haruhiko Makino Nobuaki Sato, Ichiro Muto, Katsuyoshi Hatakeyama, And Kenichi Tanaka	The prevalence of hereditary breast/ovarian cancer risk in patients with a history of breast or ovarian Cancer in Japanese subjects	J Obstet Gynecol Res	35(5)	912-917	2010
Saeki T., et al.,	Pharmacokinetic analysis of a combined chemoendocrine treatment with paclitaxel and toremifene for metastatic breast cancer.	Breast Cancer	16	113-120	2009
Saeki T., et al.,	Evaluation of the safety and tolerability of oral TAS-108 in postmenopausal patients with metastatic breast cancer.	Annals of Oncology	20(5)	868-873	2009
Saeki T., et al.,	Physiological and oncogenic aurora-pathway.	International Journal of Biological Sciences	5(7)	722-726	2009
Okita A., Saeki T., et al.	Efficacy and tolerability of weekly paclitaxel combination with high-dose toremifene citrate in patients with metastatic breast cancer.	Acta Medica Okayama	63(4)	187-194	2009
Omokawa Y., Saeki T., et al.,	In vitro and in vivo anti-tumor effects of novel Span 80 vesicles containing immobilized Eucheuma serra agglutinin.	International Journal of Pharmaceutics,		in press,	2010
Sekigawa T, Tajima A, Hasegawa T, Hasegawa Y, Inoue H, Sano Y, Matsune S, Kurono Y, Inoue I.	Gene-expression profiles in human nasal polyp tissues and identification of genetic susceptibility in aspirin intolerant asthma.	Clin Exp Allergy	39	972-981	2009

Kang E-H, Yamaguchi T, Tajima A, Nakajima T, Tomoyasu Y, Watanabe M, Yamaguchi M, Park S-B, Maki K, Inoue I.	Association of the growth hormone receptor gene polymorphisms with mandibular height in a Korean population.	*Arch Oral Biol*	54	556-562	2009
Tomoyasu Y, Yamaguchi T, Tajima A, Nakajima T, Inoue I, Maki K.	Further evidence for an association between mandibular height and the growth hoemone receptor genes in a Japanese population.	Am J Orthod Dentofacial Orthop	136	536-541	2009
Koike A, Nishida N, Inoue I, Tsuji S, Tokunaga K.	Genome-wide association database developed in the Japanese Integrated Database Project.	J Hum Genet	54	543-546	2009
Brookes AJ, Lehvaslaiho H, Muilu J, Shigemoto Y, Oroguchi T, Tomiki T, Mukaiyama A, Konagaya A, Kojima T, Inoue I, Kuroda M, Mizushima H, Thorisson GA, Dash D, Rajeevan H, Darlison MW, Woon M, Fredman D, Smith AV, Senger M, Naito K, Sugawara H.	The phenotype and genotype experiment object model (PaGE-OM): a robust data structure for information related to DNA variation.	Hum Mutat	30	968-977	2009
Nakaoka H, Inoue I.	Meta-analysis of genetic association studies: methodologies, between-study heterogeneity and winner's curse.	J Hum Genet	54	615-623	2009

Yoshihara K, Tajima A, Yahata T, Kodama S, Fujiwara H, Suzuki M, Onishi Y, Hatae M. Sueyoshi K, Fujiwara H, Kudo Y, Kotera K, Masuzaki H, Tashiro H, Katabuchi H, Inoue I, Tanaka K.	Gene expression profile for predicting survival in advanced-stage serous ovarian cancer across two independent databases.	PLoS ONE	5	e9615	2010

doi:10.1111/j.1447-0756.2009.01054.x J. Obstet. Gynaecol. Res. Vol. 35, No. 5: 1000–1003, October 2009

Extranodal Rosai–Dorfman disease involving bilateral ovaries in a patient with a ventriculoperitoneal shunt

Masayuki Yamaguchi[1], Tetsuro Yahata[1], Kazuyuki Fujita[1], Junko Sakurada[2], Go Hasegawa[2], Hajime Umezu[2], Makoto Naito[2] and Kenichi Tanaka[1]

Departments of [1]Obstetrics and Gynecology and [2]Cellular and Molecular Pathology, Niigata University Graduate School of Medical and Dental Sciences, Niigata City, Niigata, Japan

Abstract

Rosai–Dorfman disease (RDD) is a rare condition of unknown etiology, and female genital tract involvement in RDD is uncommon. We describe the first case of RDD with bilateral ovarian involvement in a patient implanted with a ventriculoperitoneal (VP) shunt. The patient was a 17-year-old Japanese woman who had undergone radiotherapy, surgery for extranodal RDD involving the brain, and VP shunt insertion at age 12. Bilateral pelvic masses were incidentally detected on a computed tomography scan. She underwent laparotomy for lesion extirpation. On abdominal washing cytology, histiocytes showing emperipolesis were identified. Bilateral salpingo-oophorectomy was performed instead of extirpation, as it was difficult to identify the lesion margins. At 24 months after surgery, the patient is well and has not developed local recurrence. Thus, RDD can recur because of implantation of lesion cells into the abdominal cavity through a VP shunt, as is observed in the case of cerebral neoplasms.

Key words: ovarian mass, Rosai–Dorfman disease, VP shunt.

Introduction

Rosai–Dorfman disease (RDD) or sinus histiocytosis with massive lymphadenopathy was first described by Rosai and Dorfman in 1969.[1] It is characterized by massive painless cervical lymphadenopathy, low-grade fever, leukocytosis, increased erythrocyte-sedimentation rate, and polyclonal hypergammaglobulinemia. The mean age at onset is reported to be 20.6 years with a male : female incidence ratio of 1.4:1.[2] Extranodal involvement is present in approximately 43% of cases, and the commonly involved sites are the skin, upper respiratory tract, bone, orbit, paranasal sinuses, the central nervous system (CNS) etc.[3] Involvement of the female genital tract is extremely rare, with only one reported case of uterine cervical involvement.[4] Microscopic features of the involved lymph nodes are perinodal fibrosis and expanded sinuses with non-neoplastic proliferation of histiocytes. These histiocytes are immunoreactive for S-100 protein, CD14, CD68, and vimentin but negative for CD1a. Lymphocytophagocytosis or emperipolesis is a characteristic finding of the disease.

The etiology, pathogenesis, and natural history of RDD are unknown. At present, this condition is considered as a benign or reactive proliferation that undergoes spontaneous regression. In contrast, extranodal RDD often mimics a malignant tumor.[5] Patients may develop recurrence or progressive disease, and multi-organ involvement has been reported. We discuss the first case of a young female patient with a history of intracranial RDD who presented with ovarian involvement, possibly associated with a ventriculoperitoneal (VP) shunt placed at the time of

Received: August 27 2008.
Accepted: December 19 2008.
Reprint request to: Dr Tetsuro Yahata, Department of Obstetrics and Gynecology, Niigata University Graduate School of Medical and Dental Sciences, 1-757, Asahimachi-dori, Chuo Ward, Niigata City, Niigata 951-8510, Japan. Email: yahatat@med.niigata-u.ac.jp

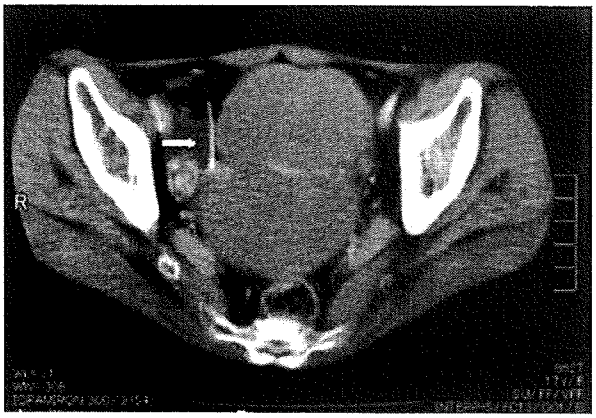

Figure 1 A computed tomography scan showing pelvic masses. The ventriculoperitoneal shunt is indicated by an arrow.

resection of the primary meningeal lesion 5 years previously.

Case Report

The patient was a 17-year-old Japanese woman with a history of radiation therapy and surgical resection of a primary meningeal lesion and VP shunt insertion at the age of 12. The results of pathological examination of the tumor led to a diagnosis of RDD. The patient was administered additional radiation therapy for multiple recurrent lesions in the spinal cord at ages 13 and 16. She had been doing well until February 2006, when she presented to a hospital with a slight fever and general fatigue. Hematological examination revealed elevation of the C-reactive protein (CRP) level (13.3 mg/dL) without leukocytosis. Meningitis was suspected, but an examination of the cerebrospinal fluid disclosed no abnormality. Despite the administration of panipenem/betamipron, the CRP level remained elevated. In order to identify the infectious focus, a systemic computed tomography (CT) scan was obtained, and incidental pelvic masses were observed in close proximity to the VP shunt catheter (Fig. 1).

Subsequently, the patient was referred to our hospital for further evaluation and treatment of the pelvic masses. At the first visit to our hospital, she complained of abdominal distension and polyuria. On pelvic examination, bilateral mobile pelvic masses were noted, and a magnetic resonance (MR) image showed 7- and 8-cm-wide solid masses that were located side-by-side, were well demarcated, and had smooth surfaces. The intensity of the masses was low on T1-weighted MR images and intermediate on T2-weighted MR images; the masses were well enhanced on contrast-enhanced MR images (Fig. 2). The levels of tumor markers such as carcinoembryonic antigen, CA-125, CA19-9, and alpha-fetoprotein were all within normal limits. The radiological differential diagnoses, determined on the basis of the finding of solid and well-demarcated masses, were fibroma, thecoma, leiomyoma etc. A diagnosis of extranodal RDD with bilateral ovarian involvement was made because the masses were similar to the previous meningeal lesion, particularly with regard to the signal intensities on MR imaging. Laparotomy for the extirpation of the lesion with preservation of the normal ovarian tissue was planned. Intraoperative exploration revealed solid, mobile, bilateral ovarian masses. Abdominal washing cytology revealed the presence of histiocytes with evidence of emperipolesis (Fig. 3). Bilateral salpingo-oophorectomy was performed as it was difficult to recognize the boundary between the lesion and the normal ovarian tissue, and to perform extirpation. The final pathological review of the specimen confirmed the results of the intraoperative frozen-section examination of the affected tissues of both ovaries: mononuclear and multinuclear polygonal histiocytes with evidence of emperipolesis were seen (Fig. 4), and the specimen was positive for S-100 protein and CD68. The patient was discharged 10 days after the surgery when her CRP level was normal; she was prescribed estrogen-replacement therapy. She has been doing well and has not shown any evidence of local recurrence for 24 months after surgery.

Discussion

While more than 600 cases of RDD have been reported, we believe this is the first reported case of extranodal RDD involving the ovaries. It is possible that the ovarian involvement was caused by implantation of the cells from the lesion in the CNS via the VP shunt because histiocytes were present in the abdominal washing cytological specimens, and this may have led to intra-abdominal relapse of RDD. When a VP shunt is placed for the management of hydrocephalus and viable cells of any type from the lesion in the CNS are present in the cerebrospinal fluid, a potential pathway is created for implantation of these cells through the shunt to the abdomen.

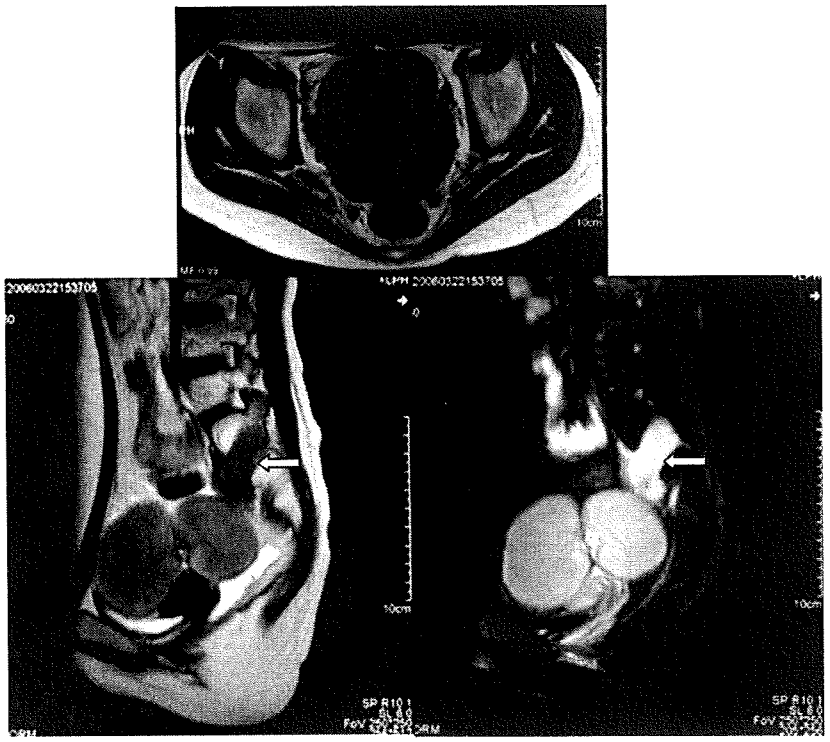

Figure 2 A magnetic resonance image showing pelvic masses. Top: T1-weighted axial image; left: T2-weighted sagittal image; and right: contrast-enhanced sagittal image. The sacral lesion, which was irradiated when the patient was 16, was one of the multiple recurrent lesions in the spinal cord (indicated by an arrow).

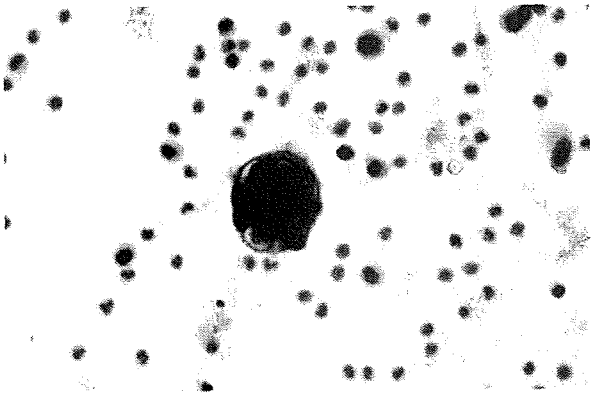

Figure 3 Photomicrograph of abdominal washing cytological specimen. Histiocytes exhibiting emperipolesis are seen (Giemsa stain, original magnification ×400).

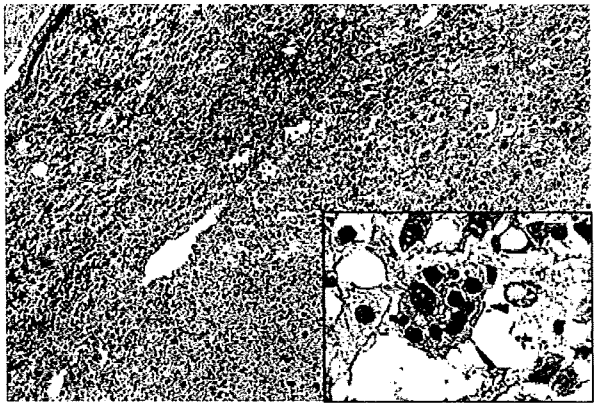

Figure 4 Histopathology slide of the ovarian tumor showing solid growths consisting of mononuclear and multinuclear polygonal histiocytes (hematoxylin and eosin stain, original magnification ×100). Emperipolesis is indicated by an arrowhead (inset, original magnification ×400).

Indeed, VP shunt-related abdominal metastases have been reported for many types of brain neoplasms, including medulloblastoma and other primitive neuroectodermal tumors, astrocytoma, germinoma, oligodendroglioma, ganglioglioma, ependymoma and melanoma.[6] However, VP shunt-related recurrence of RDD has not been reported before. Thus, it is possible that RDD recurred because of implantation of lesion cells into the abdominal cavity through the VP shunt – a phenomenon that has been observed in the case of other cerebral neoplasms.

Radiotherapy for RDD has been reported to show limited efficacy, while chemotherapy is in general ineffective.[7] Surgical resection is considered necessary in patients with impaired function of vital organs and/or with extranodal localization manifesting as important clinical signs. RDD generally has a favorable prognosis, but some patients have a chronic course with stable or progressive disease. In contrast to RDD involving a single lymph node region, RDD involving extranodal or multiple sites usually has a protracted course. It has been reported that when the surgical margins are involved, local recurrence is likely. This suggests that surgery with disease-free margins is crucial for locoregional control.[8,9] In our case, the preservation of normal ovarian tissue was difficult, and oophorectomy was performed to avoid local recurrence. However, extirpation of the lesion should be considered when appropriate and technically feasible.

This case illustrates the importance of considering metastatic disease in a patient in whom a VP shunt has been implanted. Doctors should keep in mind that RDD might recur because of implantation of lesion cells into the abdominal cavity through a VP shunt, as is known to occur in the case of cerebral neoplasms.

References

1. Rosai J, Dorfman RF. Sinus histiocytosis with massive lymphadenopathy: A newly recognized benign clinicopathological entity. *Arch Pathol* 1969; **87**: 63–70.
2. Foucar E, Rosai J, Dorfman R. Sinus histiocytosis with massive lymphadenopathy (Rosai–Dorfman disease): Review of the entity. *Semin Diagn Pathol* 1990; **7**: 19–73.
3. Cossor F, Al-Khater AH, Doll DC. Laryngeal obstruction and hoarseness associated with Rosai–Dorfman disease. *J Clin Oncol* 2006; **24**: 1953–1955.
4. Murray J, Fox H. Rosai–Dorfman disease of the uterine cervix. *Int J Gynecol Pathol* 1991; **10**: 209–213.
5. Knox SK, Kurtin PJ, Steensma DP. Isolated splenic sinus histiocytosis (Rosai–Dorfman disease) in association with myelodysplastic syndrome. *J Clin Oncol* 2006; **24**: 4027–4028.
6. Donovan DJ, Prauner RD. Shunt-related abdominal metastases in a child with choroid plexus carcinoma: Case report. *Neurosurgery* 2005; **56**: E412; discussion E412.
7. Pulsoni A, Anghel G, Falcucci P *et al.* Treatment of sinus histiocytosis with massive lymphadenopathy (Rosai–Dorfman disease): Report of a case and literature review. *Am J Hematol* 2002; **69**: 67–71.
8. Brenn T, Calonje E, Granter SR *et al.* Cutaneous Rosai–Dorfman disease is a distinct clinical entity. *Am J Dermatopathol* 2002; **24**: 385–391.
9. Cheng SP, Jeng KS, Liu CL. Subcutaneous Rosai–Dorfman disease: Is surgical excision justified? *J Eur Acad Dermatol Venereol* 2005; **19**: 747–750.

Gene expression profiling of advanced-stage serous ovarian cancers distinguishes novel subclasses and implicates *ZEB2* in tumor progression and prognosis

Kosuke Yoshihara,[1,10] Atsushi Tajima,[2,10] Dai Komata,[1] Tadashi Yamamoto,[3] Shoji Kodama,[4] Hiroyuki Fujiwara,[5] Mitsuaki Suzuki,[5] Yoshitaka Onishi,[6] Masayuki Hatae,[6] Kazunobu Sueyoshi,[7] Hisaya Fujiwara,[8] Yoshiki Kudo,[8] Ituro Inoue[2,9] and Kenichi Tanaka[1,9]

[1]Department of Obstetrics and Gynecology, Niigata University Graduate School of Medical and Dental Sciences, Niigata; [2]Department of Molecular Life Science, Tokai University School of Medicine, Isehara, Japan; [3]Department of Structural Pathology, Institute of Nephrology, Niigata University Graduate School of Medical and Dental Sciences; [4]Department of Gynecology, Niigata Cancer Center Hospital, Niigata; [5]Department of Obstetrics and Gynecology, Jichi Medical University, Shimotuke; [6]Department of Obstetrics and Gynecology, Kagoshima City Hospital; [7]Department of Pathology, Kagoshima City Hospital, Kagoshima; [8]Department of Obstetrics and Gynecology, Hiroshima University Graduate School of Biomedical Sciences, Hiroshima, Japan

(Received January 30, 2009/Revised April 16, 2009/Accepted April 24, 2009/Online publication May 26, 2009)

To elucidate the mechanisms of rapid progression of serous ovarian cancer, gene expression profiles from 43 ovarian cancer tissues comprising eight early stage and 35 advanced stage tissues were carried out using oligonucleotide microarrays of 18 716 genes. By non-negative matrix factorization analysis using 178 genes, which were extracted as stage-specific genes, 35 advanced stage cases were classified into two subclasses with superior (n = 17) and poor (n = 18) outcome evaluated by progression-free survival (log rank test, P = 0.03). Of the 178 stage-specific genes, 112 genes were identified as showing different expression between the two subclasses. Of the 48 genes selected for biological function by gene ontology analysis or Ingenuity Pathway Analysis, five genes (*ZEB2*, *CDH1*, *LTBP2*, *COL16A1*, and *ACTA2*) were extracted as candidates for prognostic factors associated with progression-free survival. The relationship between high *ZEB2* or low *CDH1* expression and shorter progression-free survival was validated by real-time RT-PCR experiments of 37 independent advanced stage cancer samples. *ZEB2* expression was negatively correlated with *CDH1* expression in advanced stage samples, whereas *ZEB2* knockdown in ovarian adenocarcinoma SKOV3 cells resulted in an increase in *CDH1* expression. Multivariate analysis showed that high *ZEB2* expression was independently associated with poor prognosis. Furthermore, the prognostic effect of E-cadherin encoded by *CDH1* was verified using immunohistochemical analysis of an independent advanced stage cancer samples set (n = 74). These findings suggest that the expression of epithelial–mesenchymal transition-related genes such as *ZEB2* and *CDH1* may play important roles in the invasion process of advanced stage serous ovarian cancer. (*Cancer Sci* 2009; 100: 1421–1428)

The serous type, comprising approximately 50% of ovarian cancers, is the most aggressive histology and has a tendency to be detected as advanced stage at the time of diagnosis.[1,2] Patients with advanced stage serous ovarian cancer are managed with surgical cytoreduction followed by platinum and taxane-based chemotherapy. Serous ovarian cancer is moderately chemosensitive and initially responds to postoperative chemotherapy, but the survival of patients with advanced stage remains poor. Because the majority of early stage ovarian cancers are asymptomatic and there is as yet no reliable screening test, it is difficult to diagnose early stage serous ovarian cancer. Therefore, the molecular mechanisms of progression in serous ovarian cancer should provide valuable clues for early detection and improved prognosis.

The development of microarray technology permits analysis of the expression levels of thousands of genes in cancer cells, and several studies have shown that microarrays can be used to identify gene expression profiles associated with surgery outcome, response to chemotherapy, grade, and survival in ovarian cancers.[3–17] However, there are limited reports of microarray analysis on tumor progression.[18–20] Serous ovarian cancer more rapidly progresses to advanced stage than other histological types.[21] In the present study, we used genome-wide expression microarray to distinguish between stage I (ovary confined) and stage III/IV serous ovarian cancers to focus on the molecular mechanisms of tumor progression and metastasis. Our microarray analysis identified 178 stage-specific genes, and also divided advanced stage (stage III/IV) ovarian cancers into two novel prognostic subclasses, by the NMF method. There were significant differences between the two subclasses in progression-free survival time. Furthermore, we extracted *CDH1* and its transcriptional repressor *ZEB2* from the 112 genes that were differentially expressed between the two novel subclasses, and found that the expression levels of these epithelial–mesenchymal transition-related genes[22,23] are associated with tumor progression and prognosis in advanced stage serous ovarian cancer patients.

Materials and Methods

Tissue samples. Eighty-nine patients (17 stage I; 72 stage III/IV) who were diagnosed with serous histological type ovarian cancer between July 1997 and October 2007 were recruited in this study. Fresh-frozen samples were obtained from primary tumor tissues at initial cytoreductive surgery. No patients received chemotherapy before surgery. All patients with advanced stage serous ovarian cancer (n = 72) were treated with platinum and taxane-based chemotherapy after surgery. The ethics committees of the participating institutions approved the study protocol, and each participant gave written, informed consent. Of the 89 samples, 43 were analyzed with microarray. The remaining 46 samples were used for subsequent validation analysis. There were no significant differences between the two samples sets regarding age of onset, stage, performance of optimal cytoreduction, histological grade, and follow-up period between the microarray set and validation set (Supplementary Table 1). Staging of the disease was assessed in accordance with the criteria of the International Federation of Gynecology and Obstetrics.[24] Optimal cytoreduction was defined as ≤1 cm of gross residual disease. The histological characteristics of surgically resected specimens

[9]To whom correspondence should be addressed.
E-mail: tanaken@med.niigata-u.ac.jp or ituro@is.icc.u-tokai.ac.jp
[10]These authors contributed equally to this work.

doi: 10.1111/j.1349-7006.2009.01204.x

were assessed on formalin-fixed and paraffin-embedded hematoxylin–eosin sections, and frozen tissues containing more than 80% tumor cells were used for RNA extraction. Normal peritoneum tissues were obtained from 10 patients having other procedures (such as hysterectomy for myoma uteri) at Niigata University. Tumors of 43 samples used for microarray analysis were screened for the presence of *TP53* somatic mutations using previously reported methods.[25] Four patients with family history of ovarian cancer in the microarray set were examined for germline mutations of *BRCA1* according to an in-house protocol,[26] and two patients showed mutations of *BRCA1*.

Microarray experiments. Total RNA, extracted from tissue samples using TRIzol reagent (Invitrogen, Carlsbad, CA, USA) was examined with a 2100 Bioanalyzer (Agilent Technologies, Palo Alto, CA, USA) using an RNA 6000 Nano LabChip (Agilent Technologies). Five hundred nanograms of total RNA was converted into labeled cRNA with nucleotides coupled to Cy3 (PerkinElmer, Boston, MA, USA) using the Low RNA Input Fluorescent Linear Amplification Kit (Agilent Technologies). Cy3-labeled cRNA (1.5 μg) was hybridized for 17 h at 65°C to an Agilent Human 1A (v2) Oligo Microarray, which carries 60-mer probes to 18 716 human transcripts. The hybridized microarray was washed and then scanned in Cy3 channel with the Agilent DNA Microarray Scanner (model G2565AA). Signal intensity per spot was generated from the scanned image with Feature Extraction Software version 8.5 (Agilent Technologies) with the default settings. Spots that did not pass quality control procedures were flagged as 'absent'.

Microarray data analysis. Data normalization was carried out using GeneSpring GX 7.3 (Agilent Technologies) as follows: (i) values below 0.01 were set to 0.01, following background subtraction; and (ii) median percentile normalization was carried out using a per-chip 50th percentile of all measurements. Furthermore, genes with expression levels marked as 'absent' in more than 22 of 43 microarrays were excluded to analyze ovarian cancer-specific transcripts. When the gene expression patterns of two groups were compared, genes showing twofold or more mean expression differences between the groups were first determined by Welch's *t*-test in GeneSpring GX. For multiple testing corrections in this statistical analysis, the Benjamini–Hochberg procedure[27] of controlling the false discovery rate at the level of 0.05 was used.

To assess heterogeneity of the gene expression profile among serous ovarian cancer patients, we applied a NMF algorithm and hierarchical clustering using stage-specific gene expression profiles. NMF analysis was carried out according to Brunet *et al.*[28] as previously reported.[29]

To investigate the biological functions of the gene expression profiles, we used GO Ontology Browser, embedded in GeneSpring GX, and IPA (http://www.ingenuity.com). More detailed information about this analysis using the GO Ontology Browser and IPA is given in Supplementary methods.

Quantitative RT-PCR analysis. Total RNA (1 μg) from ovarian cancer was used as a template in first-strand cDNA synthesis with the SuperScript III First-Strand Synthesis System (Invitrogen). The cDNA was diluted one in ten for subsequent real-time PCR, which was carried out using TaqMan Gene Expression Assays (Applied Biosystems) with TaqMan Universal PCR Master Mix (Applied Biosystems) on a 7900HT Sequence Detection System (Applied Biosystems) according to the manufacturers' instructions. Detailed information on the 23 transcripts examined is summarized in Supplementary Table 2. The relative quantification method[30] was used to measure the amounts of the respective genes in serous ovarian cancer samples, normalized to *ACTB* and *TBP*.

Analysis of clinical and pathological parameters. All analyses except Cox's proportional hazard analysis were done using GraphPad PRISM version 4.0 (GraphPad Software, San Diego, CA, USA). Survival curves were investigated using the Kaplan–Meier method and log rank test (GraphPad PRISM). When clinicopathological parameters among ovarian cancer patients were compared, unpaired *t*-test, Fisher's exact test or χ^2-test was used depending on the purpose (GraphPad PRISM). Pearson's correlation coefficient was calculated for correlation between *ZEB2* expression and *CDH1* expression. Differences in gene expression levels between two subclasses were tested by Mann–Whitney test. Using a $\log_2$ transformation of expression data, Cox's proportional hazard model analysis was carried out using JMP version 6 (SAS Institute, Cary, NC, USA).

Results

Identification and characterization of molecular subclasses from advanced stage serous ovarian cancer cases. Using Agilent Human 1A(v2) Oligo microarray, we generated gene expression data for 43 serous ovarian cancers comprising eight stage I and 35 stage III/IV tumors, as well as 10 normal peritoneum tissues as a reference. First, 4275 ovarian cancer-specific genes that were differentially expressed between ovarian cancer and peritoneum tissues were isolated. Of these 4275 transcripts, 178 stage-specific genes showing significantly more than twofold upregulation or downregulation in stage III/IV samples compared to stage I samples; 107 transcripts were upregulated and 71 transcripts downregulated in stage III/IV serous ovarian cancers (Supplementary Fig. 1).

To clarify the heterogeneity of the samples at the transcriptome level, 43 serous ovarian cancer samples were analyzed by the NMF method[28,29,31] using the 178 transcriptomes that were differentially expressed between stage I samples and stage III/IV samples. Figure 1(A) shows reordered consensus matrices averaging 50 connective matrices generated for subclasses $K = 2$, 3, 4, and 5. The most distinct pattern of block partitioning was observed at the $K = 2$ model. Thus, the NMF method predicts the existence of robust subclasses of serous ovarian cancer samples for $K = 2$. This prediction was quantitatively supported by higher values of coph for NMF-clustered matrices. The NMF class assignment for $K = 2$ was the most robust with the highest coph value (coph = 0.999). Interestingly, one subclass in the $K = 2$ model was composed of eight stage I samples and 17 stage III/IV samples, whereas the other was composed of 18 stage III/IV samples. To verify the accuracy and robustness of the classification, a hierarchical clustering approach was also applied to log-transformed normalized data for stage-specific target genes. As depicted in Figure 1(B), 43 serous ovarian cancer samples were separated into two main branches showing similarity with the NMF-based subclassification. Thus, it was confirmed that the 35 advanced stage serous ovarian cancer samples were categorized into two distinct subclasses at the transcriptome level. A group composed of 17 stage III/IV samples with gene expression profiles similar to stage I samples was termed 'subclass 1', and the second group comprising 18 stage III/IV samples was termed 'subclass 2'. Two patients were identified as harboring *BRCA1* mutations: one patient belonged to stage I and the other to subclass 1 in the array analysis, but there was no particular gene expression pattern due to the mutations based on the expression levels of the 178 stage-specific genes.

We then investigated the possibility that the two subclasses of advanced stage serous ovarian cancers split by the NMF approach might represent clinically, pathologically, or genetically distinct characteristics. The distribution of several known prognostic factors is listed in Table 1. The two subclasses were similar in age of onset, stage, CA125 level before treatment, presence of tumor cells in ascites, histological grade, presence of lymph node metastasis, and frequency of *TP53* mutations, except that subclass 1 had a higher rate of optimal cytoreduction than subclass 2 (Fisher's exact test, $P = 0.09$). When the outcome of two

doi: 10.1111/j.1349-7006.2009.01204.x

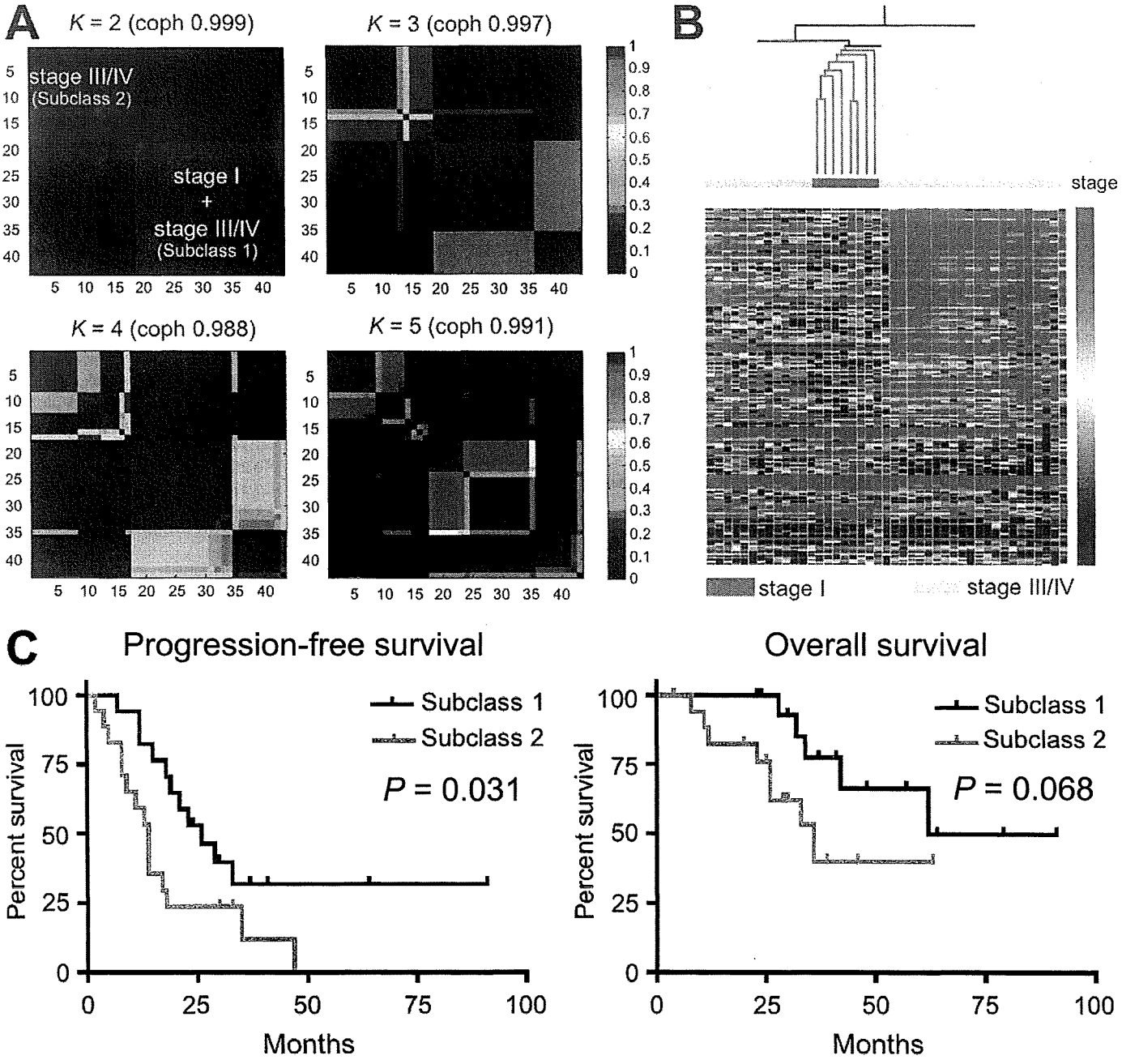

Fig. 1. Subclassification of 43 serous ovarian cancer samples and their prognosis. (A) By a non-negative matrix factorization (NMF) approach, NMF-consensus matrices averaging 50 connectivity matrices were computed at $K = 2$–5 (as the number of subclasses modeled) for the 43 serous ovarian cancer samples with 178 stage-specific genes. The NMF computation and model selection were carried out according to Brunet *et al.*[28] By accounting for the cophenetic correlation coefficients (coph) for NMF-clustered matrices, the NMF class assignment at $K = 2$ was the most robust. One subclass in the $K = 2$ model contained samples both from stage I ($n = 8$) and III/IV ($n = 17$), whereas the other contained only stage III/IV samples ($n = 18$). (B) A hierarchical clustering method was also used to classify serous ovarian cancer samples using 178 stage-specific genes. The 43 serous samples were largely separated into two clusters. The stage assignments for samples are: stage I, red; and stage III/IV, yellow. (C) Kaplan–Meier survival curves between two NMF-based subclasses of the 35 stage III/IV patients. Subclass 1, composed of 17 advanced stage patients with gene expression profiles similar to that of stage I, showed statistically prolonged progression-free survival (log rank test, $P = 0.031$), but no significant correlation with overall survival (log rank test, $P = 0.068$).

subclasses was compared for progression-free survival and overall survival, the Kaplan–Meier curves showed significantly better outcome in cases belonging to subclass 1 in progression-free survival (Fig. 1C, log rank test, $P = 0.031$) and fair outcome in overall survival (Fig. 1C, log rank test, $P = 0.068$).

Association of subclass-specific gene expression profile with prognosis of ovarian cancer patients. To characterize the gene expression differences associated with distinct prognoses between the two subclasses of advanced stage serous ovarian cancers, we identified 112 subclass-specific transcripts that were differentially expressed between the two subclasses; 25 transcripts were up-regulated in subclass 1 and 87 transcripts were upregulated in subclass 2 (Supplementary Table 3). We then examined the biological functions of the 112 subclass-specific genes using two analytic tools, GO analysis and IPA, to clarify the biological mechanism of tumor progression. The Gene Ontology Biological

Table 1. Clinical characteristics of two subclasses of advanced stage serous ovarian cancer samples

Characteristic	Subclass 1 ($n = 17$)	Subclass 2 ($n = 18$)	*P*-value
Age (years)	58.5 ± 8.6	61.1 ± 12.6	0.49†
Stage			
Stage III	16	15	1‡
Stage IV	1	3	
CA125 (IU)	1987 ± 2021	1178 ± 1057	0.14†
Cancer cell in abdominal fluid			
Positive	15	15	1‡
Negative	2	3	
Optimal cytoreduction			
Optimal (<1 cm)	12	7	0.09‡
Not optimal	5	11	
Lymph node metastasis			
Positive	6	4	1‡
Negative	9	6	
Unknown	2	8	
Grade			
Grade 1	6	4	0.18§
Grade 2	9	7	
Grade 3	2	7	
TP53 status			
Wild type	11	9	0.50‡
Mutated	6	9	

Differences in clinical characteristics between subclass 1 and subclass 2 were tested using the †unpaired *t*-test, ‡Fisher's exact test or §χ^2-test.

Table 2. Univariable Cox's proportional hazards model analysis of expression levels of five genes for progression-free survival and overall survival in patients with advanced stage serous ovarian cancers

Gene symbol	Hazard ratio (95% CI)	*P*-value
Microarray set (n = 35)		
Progression-free survival		
ZEB2	1.35 (1.06–1.77)	0.015*
CDH1	0.75 (0.62–0.94)	0.017*
LTBP2	1.63 (1.04–2.57)	0.032*
COL16A1	1.33 (1.02–1.74)	0.034*
ACTA2	1.21 (1.01–1.46)	0.036*
Overall survival		
ZEB2	1.56 (1.06–2.47)	0.023*
CDH1	0.81 (0.67–1.03)	0.081
LTBP2	2.53 (1.43–4.58)	0.0017*
COL16A1	1.66 (1.12–2.59)	0.012*
ACTA2	1.44 (1.10–1.95)	0.0087*
Validation set (n = 37)		
Progression-free survival		
ZEB2	1.74 (1.08–2.92)	0.023*
CDH1	0.20 (0.09–0.45)	0.00006*
LTBP2	1.16 (0.75–1.75)	0.49
COL16A1	1.18 (0.92–1.51)	0.20
ACTA2	1.22 (0.90–1.66)	0.19
Overall survival		
ZEB2	1.89 (1.06–3.64)	0.029*
CDH1	0.59 (0.26–1.30)	0.19
LTBP2	1.1 (0.70–1.66)	0.69
COL16A1	1.23 (0.93–1.66)	0.15
ACTA2	1.43 (0.99–2.13)	0.052

*$P < 0.05$.

Process categories over-represented among 112 subclass-specific genes are shown in Figure 2(A). After multiple testing corrections using the Benjamini–Hochberg FDR method, seven categories were significantly over-represented, and included 37 non-overlapping genes. Subclass-specific genes were involved in biological processes of transport (GO6817, GO15698, GO6820, and GO6811), development (GO48513 and GO1501), and cell adhesion (GO7155), and included a high proportion of extracellular matrix-related genes. In addition, when ID of Agilent probes of 112 subclass-specific transcripts were imported into the IPA software, a new pathway comprising 26 genes that were enriched in extracellular matrix genes was identified (Fig. 2B). Fifteen genes belonged to both the seven GO categories and the new network, and 48 non-redundant genes were biologically characterized.

To investigate whether the expression profile of the 48 genes extracted by GO analysis or IPA was implicated in the aggressive phenotype of ovarian cancer, we analyzed the association between the respective expression levels of the 48 genes and progression-free survival time using univariate Cox's proportional hazard model. The expression levels of *ZEB2*, *CDH1*, *LTBP2*, *COL16A1*, and *ACTA2* were significantly correlated with progression-free survival (Table 2). When overall survival also was evaluated by Cox's proportional hazard model, the expression of the above genes except *CDH1* was significantly correlated with overall survival.

Validation by quantitative real-time RT-PCR. To validate the microarray expression data, we measured expression levels of 23 randomly selected transcripts from the 112 subclass-specific transcripts by real-time RT-PCR analysis. In agreement with microarray results, there was a significant difference between the expression levels of the 23 transcripts measured by real-time RT-PCR of subclass 1 and subclass 2 (Supplementary Table 4).

To validate the previous findings that the expression levels of *ZEB2*, *CDH1*, *LTBP2*, *COL16A1*, and *ACTA2* are associated with progression-free survival, quantitative real-time RT-PCR was carried out on 46 samples comprising nine stage I samples and 37 stage III/IV samples recruited as an independent validation set. Cox's proportional hazard analysis showed that the expression levels of *ZEB2* and *CDH1* were again correlated with progression-free survival ($P = 0.023$ and 0.00006, respectively) (Table 2). Moreover, *ZEB2* expression was significantly associated with overall survival ($P = 0.029$). At the protein level, an association of the expression of E-cadherin (encoded by *CDH1*) with prognosis of advanced stage serous ovarian cancer patients was further verified by immunohistochemical analysis of independent samples ($n = 74$) (Supplementary Fig. 3) as previously reported.[32–35]

Interaction between *ZEB2* and *CDH1*. *ZEB2* directly interacted with *CDH1* in the IPA network, as shown in Figure 2(B). We also found a significantly negative correlation between *ZEB2* expression and *CDH1* expression (Pearson's correlation coefficient: –0.432, $P = 0.0002$) in advanced stage serous ovarian cancers using real-time RT-PCR data ($n = 72$). *ZEB2* acts on the promoter of *CDH1*, a well-known epithelial marker, and reduces its expression.[23,36] To confirm the interaction between *ZEB2* and *CDH1* in ovarian cancer cells, a siRNA approach was used. For this purpose, we selected the SKOV3 cell line expressing endogenously higher *ZEB2* and lower *CDH1* mRNA than other ovarian cancer cell lines (Supplementary Fig. 3A,B). In SKOV3 cells, siRNA-mediated transient silencing of *ZEB2* expression resulted in upregulation of *CDH1* expression and downregulation of *FN1* and *VIM* expression (Supplementary Fig. 3C–F).

For multivariate analysis, we selected *ZEB2* from the two genes as likely to be the more important prognostic factor owing to its functional significance as an upstream repressor of *CDH1*.[23] The prognostic capability of *ZEB2* was further compared with other prognosis-related variables such as clinicopathological factors including age, performance of optimal cytoreduction, and histological grade using multivariate Cox's proportional

doi: 10.1111/j.1349-7006.2009.01204.x

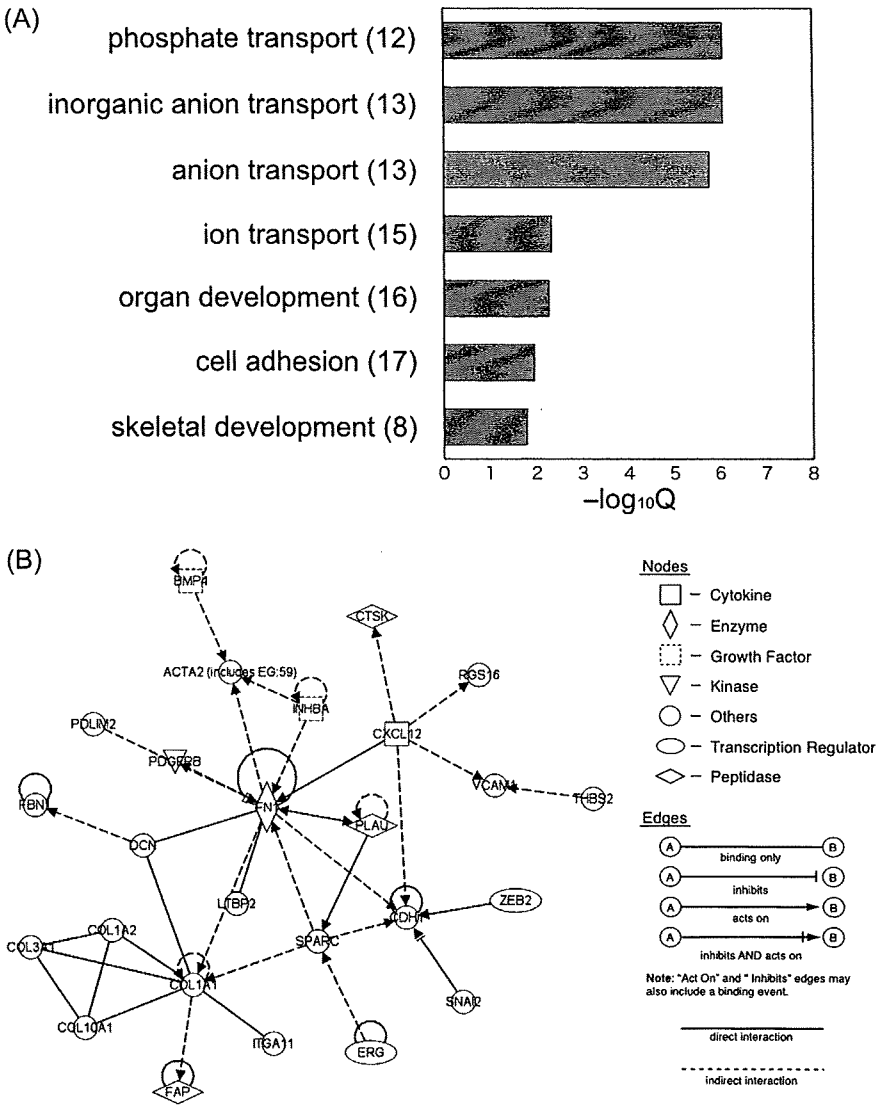

Fig. 2. Biological characterization of 112 subclass-specific genes using Gene Ontology analysis and Ingenuity Pathway Analysis (IPA). (A) Significant enrichments of gene ontology (GO) categories in GO-based profiling of 112 subclass-specific genes. Gray bars represent *q*-values (expressed as the negative logarithm [base 10]) after multiple testing correction of the Benjamini–Hochberg false discovery rate method for the significant ($q < 0.05$) GO categories over-represented in the 112 subclass-specific genes, using 4275 ovarian cancer-specific genes as a background set of genes for the determination of *q*-values. The actual number of the subclass-specific genes involved in each category is given in parentheses. (B) Twenty-six of 112 (24.1%) genes appeared in a new network based on the Ingenuity Pathway Knowledge base. Nodes represent genes, with their shapes showing IPA-defined functional classes of genes, and edges indicating biological relationships between nodes.

hazards analysis (Table 3). To increase the reliability of the multivariate analyses, all of the advanced stage serous ovarian cancer samples ($n = 72$) were analyzed by the real-time PCR technique. In Cox's proportional hazards model, *ZEB2* expression and the rate of optimal cytoreduction surgery were independent factors for progression-free survival time ($P = 0.014$ and 0.0011 respectively). The hazard ratio for relapse of *ZEB2* expression was 1.37 (95% confidence interval 1.07–1.78). Furthermore, when overall survival was evaluated by multivariate analysis, only the *ZEB2* expression level was independently associated with overall survival time ($P = 0.027$, hazard ratio = 1.53, 95% confidence interval 1.05–2.22).

***ZEB2* and *CDH1* expression and survival.** To clarify the details of the *ZEB2–CDH1* relationship, we analyzed the prognostic implications with regard to combinations of *ZEB2* and *CDH1* expression. For this purpose, we divided all of the samples into four groups, as shown in Table 4, when using a median expression level of each gene as a threshold for sample division. Multivariate Cox's proportional hazard model was used to compare survival among these four groups. The group showing high expression of *CDH1* and low expression of *ZEB2* served as a reference. Of the four groups, the only group with low expression of *CDH1* and high expression of *ZEB2* showed significantly poor prognosis in both progression-free survival and overall survival ($P = 0.0035$ and 0.013 respectively). When *ZEB2* expression was analyzed in combination with *CDH1* expression, the prognostic power of these genes became more significant.

Discussion

In this study, we evaluated the global gene expression profile to clarify the molecular etiology of the rapid progression specific to serous histological type cancers. We first attempted to subclassify our 43 serous type ovarian cancer tissues comprising eight stage I samples and 35 stage III/IV samples by a stepwise extraction of genes reflecting expression differences between samples (Supplementary Fig. 1). Although various classification methods have been proposed to characterize various cancer types at the molecular level using gene expression data, most of the methods tend to be unstable, producing different clusters with slightly different input or different choice of initial conditions.[37] Brunet *et al.*[28] showed that NMF is able to recover biologically significant phenotypes and appears superior to other methods especially when prior knowledge is lacking or undetermined. By applying the NMF algorithm, 35 patients with advanced stage serous ovarian cancer were grouped into two subclasses with 112 subclass-specific genes representing unique characteristics of tumor progression. Interestingly, one subclass, subclass 1 ($n = 17$), with a gene expression profile similar to that of stage I, showed a favorable outcome compared to the other subclass,